Large tuning of birefringence in two strip silicon waveguides via optomechanical motion

Jing Ma* and Michelle L. Povinelli

[1]*Ming Hsieh Department of Electrical Engineering, University of Southern California, Powell Hall of Engineering, 3737 Watt Way, Los Angeles, CA 90089-0271, USA*
**jingm@usc.edu*

Abstract: We present an optomechanical method to tune phase and group birefringence in parallel silicon strip waveguides. We first calculate the deformation of suspended, parallel strip waveguides due to optical forces. We optimize the frequency and polarization of the pump light to obtain a 9nm deformation for an optical power of 20mW. Widely tunable phase and group birefringence can be achieved by varying the pump power, with maximum values of 0.026 and 0.13, respectively. The giant phase birefringence allows linear to circular polarization conversion within 30μm for a pump power of 67mW. The group birefringence gives a tunable differential group delay of 6fs between orthogonal polarizations. We also evaluate the tuning performance of waveguides with different cross sections.

OCIS Codes: (130.3120) Integrated optics devices; (260.1440) Birefringence

References and links

1. M. L. Povinelli, M. Loncar, M. Ibanescu, E. J. Smythe, S. G. Johnson, F. Capasso, and J. D. Joannopoulos, "Evanescent-wave bonding between optical waveguides," Opt. Lett. **30**(22), 3042–3044 (2005).
2. M. L. Povinelli, M. Ibanescu, S. G. Johnson, and J. D. Joannopoulos, "Slow-light enhancement of radiation pressure in an omnidirectional-reflector waveguide," Appl. Phys. Lett. **85**(9), 1466–1468 (2004).
3. F. Riboli, A. Recati, M. Antezza, and I. Carusotto, "Radiation induced force between two planar waveguides," Eur. Phys. J. D **46**(1), 157–164 (2008).
4. M. L. Povinelli, "Microphotonics: Under pressure (News and Views)," Nat. Photonics **1**(7), 370–371 (2007).
5. M. L. Povinelli, S. G. Johnson, M. Lonèar, M. Ibanescu, E. J. Smythe, F. Capasso, and J. Joannopoulos, "High-Q enhancement of attractive and repulsive optical forces between coupled whispering-gallery- mode resonators," Opt. Express **13**(20), 8286–8295 (2005).
6. J. Ng, C. T. Chan, P. Sheng, and Z. Lin, "Strong optical force induced by morphology-dependent resonances," Opt. Lett. **30**(15), 1956–1958 (2005).
7. P. T. Rakich, M. A. Popovic, M. Soljacic, and E. P. Ippen, "Trapping, corralling and spectral bonding of optical resonances through optically induced potentials," Nat. Photonics **1**(11), 658–665 (2007).
8. H. Taniyama, M. Notomi, E. Kuramochi, T. Yamamoto, Y. Yoshikawa, Y. Torii, and T. Kuga, "Strong radiation force induced in two-dimensional photonic crystal slab cavities," Phys. Rev. B **78**(16), 165129 (2008).
9. M. Eichenfield, C. P. Michael, R. Perahia, and O. Painter, "Actuation of micro-optomechanical systems via cavity-enhanced optical dipole forces," Nat. Photonics **1**(7), 416–422 (2007).
10. M. Li, W. H. P. Pernice, C. Xiong, T. Baehr-Jones, M. Hochberg, and H. X. Tang, "Harnessing optical forces in integrated photonic circuits," Nature **456**(7221), 480–484 (2008).
11. W. H. P. Pernice, M. Li, and H. X. Tang, "Theoretical investigation of the transverse optical force between a silicon nanowire waveguide and a substrate," Opt. Express **17**(3), 1806–1816 (2009).
12. M. Li, W. H. P. Pernice, and H. X. Tang, "Tunable bipolar optical interactions between guided lightwaves," Nat. Photonics **3**(8), 464–468 (2009).
13. G. S. Wiederhecker, L. Chen, A. Gondarenko, and M. Lipson, "Controlling photonic structures using optical forces," Arxiv 0904.0794v1.
14. J. Chan, M. Eichenfield, R. Camacho, and O. Painter, "Optical and mechanical design of a "zipper" photonic crystal optomechanical cavity," Opt. Express **17**(5), 3802–3817 (2009).
15. M. Eichenfield, R. Camacho, J. Chan, K. J. Vahala, and O. Painter, "A picogram- and nanometre-scale photonic-crystal optomechanical cavity," Nature **459**(7246), 550–555 (2009).
16. S. H. Yang, M. L. Cooper, P. R. Bandaru, and S. Mookherjea, "Giant birefringence in multi-slotted silicon nanophotonic waveguides," Opt. Express **16**(11), 8306–8316 (2008).

#113783 - $15.00 USD Received 7 Jul 2009; revised 4 Sep 2009; accepted 8 Sep 2009; published 21 Sep 2009

17. C. Kerbage, P. Steinvurzel, P. Reyes, P. S. Westbrook, R. S. Windeler, A. Hale, and B. J. Eggleton, "Highly tunable birefringent microstructured optical fiber," Opt. Lett. **27**(10), 842–844 (2002).
18. C. Kerbage, and B. J. Eggleton, "Numerical analysis and experimental design of tunable birefringence in microstructured optical fiber," Opt. Express **10**(5), 246–255 (2002).
19. T. R. Wolinski, A. Czapla, S. Ertman, M. Tefelska, A. W. Domanski, E. N. Kruszelnicki, and R. Dabrowski, "Tunable highly birefringent solid-core photonic liquid crystal fibers," Opt. Quantum Electron. **39**(12-13), 1021–1032 (2007).
20. K. K. Tsia, S. Fathpour, and B. Jalali, "Electrical tuning of birefringence in silicon waveguides," Appl. Phys. Lett. **92**(6), 061109 (2008).
21. M. Kumar, T. Sakaguchi, and F. Koyama, "Wide tunability and ultralarge birefringence with 3D hollow waveguide Bragg reflector," Opt. Lett. **34**(8), 1252–1254 (2009).
22. COMSOL is a multiphysics software package for performing finite-element-method (FEM) simulations. See *http://www.comsol.com/*.
23. M. I. T. Photonic Bands, (MPB) is a free software package for the solution of the electromagnetic eigenmodes of periodic structures. MPB has been developed at MIT, *http://ab-initio.mit.edu/wiki/index.php/MPB*.
24. V. R. Almeida, Q. F. Xu, C. A. Barrios, and M. Lipson, "Guiding and confining light in void nanostructure," Opt. Lett. **29**(11), 1209–1211 (2004).
25. Q. Xu, V. R. Almeida, R. R. Panepucci, and M. Lipson, "Experimental demonstration of guiding and confining light in nanometer-size low-refractive-index material," Opt. Lett. **29**(14), 1626–1628 (2004).
26. J. D. Jackson, Classical Electromagnetics, 3rd edition, (John Wiley & Sons, New York, 1999).
27. V. A. Parsegian, *Van der Waals Forces*, (Cambridge University Press, Cambridge, 2005).
28. A. H. Rose, N. Feat, and S. M. Etzel, "Wavelength and temperature performance of polarization-transforming fiber," Appl. Opt. **42**(34), 6897–6904 (2003).
29. M. R. Watts, and H. A. Haus, "Integrated mode-evolution-based polarization rotators," Opt. Lett. **30**(2), 138–140 (2005).
30. Y. Shani, R. Alferness, T. Koch, U. Koren, M. Oron, B. I. Miller, and M. G. Young, "Polarization rotation in asymmetric periodic loaded rib waveguides," Appl. Phys. Lett. **59**(11), 1278–1280 (1991).
31. J. J. G. M. van der Tol, F. Hakimzadeh, J. W. Pedersen, D. Li, and H. van Brug, "New short and low-loss passive polarization converter on InP," IEEE Photon. Technol. Lett. **7**(1), 32–34 (1995).
32. K. Bayat, S. K. Chaudhuri, and S. Safavi-Naeini, "Ultra-compact photonic crystal based polarization rotator," Opt. Express **17**(9), 7145–7158 (2009).
33. C. Fietz, and G. Shvets, "Nonlinear polarization conversion using microring resonators," Opt. Lett. **32**(12), 1683–1685 (2007).
34. R. Manning, A. Antonopoulos, R. L. Roux, and A. Kelly, "Experimental measurement of nonlinear polarisation rotation insemiconductor optical amplifiers," Electron. Lett. **37**(4), 229–231 (2001).
35. H. Soto, D. Erasme, and G. Guekos, "Cross-polarization modulation in semiconductor optical amplifiers," IEEE Photon. Technol. Lett. **11**(8), 970–972 (1999).
36. R. W. Boyd, *Nonlinear Optics*, (2nd edition, Academic Press, Boston, 2003).
37. "Tables and graphs of the complex index of refraction for common microfabrication materials," *http://www.ee.byu.edu/photonics/tabulatedopticalconstants.phtml*
38. C. Fietz, and G. Shvets, "Simultaneous fast and slow light in microring resonators," Opt. Lett. **32**(24), 3480–3482 (2007).
39. F. Morichetti, A. Melloni, A. Breda, A. Canciamilla, C. Ferrari, and M. Martinelli, "A reconfigurable architecture for continuously variable optical slow-wave delay lines," Opt. Express **15**(25), 17273–17282 (2007).
40. F. Morichetti, C. Ferrari, A. Melloni, and M. Martinelli, "Polarization-Selective Tunable Delay in Coupled-Resonator Optical Delay-Lines," in *Integrated Photonics and Nanophotonics Research and Applications*, (Optical Society of America, 2008), paper IWG1.

1. Introduction

Optical forces have recently been investigated as a way of repositioning microphotonic elements such as waveguides [1–4] and microcavities [5–8]. In coupled waveguides or microcavities, the force can show either attractive or repulsive behavior depending on the relative phase of the incident light in each waveguide or microcavity. As a result, waveguide (or cavity) separation can be adjusted by tuning the power and/or polarization of input light.

Experiments have now demonstrated motion induced by optical forces in a variety of microphotonic systems. Eichenfield et al. [9] achieved micron-scale displacement of a micrometer-scale waveguide evanescently coupled to a high-Q optical microresonator at milliwatt optical powers. Li et al. demonstrated attractive and repulsive optical forces between a suspended waveguide and dielectric substrate, actuated by a pulsed light source [10–12]. Attractive and repulsive forces have also been observed in stacked microring structures [13], where Wiederhecker et al. achieved static displacements up to 12nm. Optomechanical modes

#113783 - $15.00 USD Received 7 Jul 2009; revised 4 Sep 2009; accepted 8 Sep 2009; published 21 Sep 2009

have been analyzed [14] and measured [15] in doubly-clamped beam structures with linear arrays of etched air holes forming optically resonant cavities. As the field of optical forces in integrated photonic devices matures, it is important to map out the novel functionalities that this relatively new form of mechanical actuation allows.

In this paper, we study the use of optical forces to achieve highly tunable birefringence in a coupled waveguide system. Birefringence refers to differences in propagation between orthogonally polarized modes. Phase birefringence, the difference between the phase indices, induces a relative phase shift between orthogonal components of incident light, which may be used for polarization rotators in optical communication systems. Group birefringence, defined as the difference between the group indices of different polarizations, leads to a polarization-dependent time delay and can be exploited to realize polarization-sensitive delay lines, splitters, and multiplexers. It has previously been observed that silicon waveguides with multiple etched slots exhibit giant birefringence behavior, with a group index difference as large as 1.5 between TE and TM polarized light [16]. The magnitude of birefringence depends on the slot width, as well as other design parameters. However, after the device is fabricated, the slot width is fixed, as is the value of the birefringence. Here, we present an optomechanically-controlled system which resembles a suspended one-slot waveguide with an adjustable slot width that depends on the optical force and exhibits highly tunable birefringence.

A variety of methods have been used to achieve tunable birefringence, including thermal and stress tuning. However, the achievable tuning range is generally small. For example, thermal tuning of polymer-filled microstructured fibers [17, 18] and photonic liquid crystal fibers [19] yields changes in birefringence on the order of 10^{-4}. For microphotonic devices, Tsia et al. [20] demonstrated dynamic control of birefringence on the order of 10^{-4} in a silicon waveguide by electrically tuning the stress on the waveguide core using an integrated piezoelectric film. Recently, Kumar et al. [21] varied the air-core thickness in a 3D hollow waveguide via MEMS acutation to offer a large birefringence of 0.012 with a tuning range of 0.01. This result points to the relatively large changes in birefringence that can be achieved using mechanical motion to physically change the waveguide geometry.

In this work, we calculate the tunable birefringence that can be achieved by using an optical force to adjust the separation between parallel, suspended, strip silicon waveguides. The force arising from the evanescent coupling between the modes of the two waveguides deforms both waveguides, changing the air-slot width. Such behavior results in all-optically adjustable giant birefringence. In Section 2, we characterize the two-waveguide system, and optimize the frequency and polarization of input light to achieve a considerable optical force at a moderate laser power. We calculate the resultant displacement of both waveguides based on the finite-element method (FEM) [22]. In Sections 3 and 4, we respectively evaluate the performance of the optimized optical force in tuning phase and group birefringence. We show that the optomechanical approach is characterized by widely tunable birefringence. We explore the applications of the two-waveguide system for tunable linear-to-circular polarization conversion and polarization-dependent delay.

2. Design method

Figure 1(a) shows two parallel silicon strip waveguides (refractive index n=3.45) separated by a distance d. Both ends of the waveguides rest on a SiO_2 substrate, with a free-standing section of length L. Each waveguide has a cross section of dimensions $w \times h$. We consider the transverse electric (TE) mode with electric field vector primarily parallel to the air slot ($\boldsymbol{E}_y$), and the transverse magnetic (TM) mode with electric field vector primarily perpendicular to the slot ($\boldsymbol{E}_z$). We first consider the case where the cross section of each waveguide is square (w=h=a). Figure 1(b) shows the dispersion relation calculated by the MIT Photonic Bands package [23] for the lowest TE and TM mode for several different separations. We only consider the guided modes lying below the light cone (yellow). The insets illustrate the $\boldsymbol{E}_y$

#113783 - $15.00 USD Received 7 Jul 2009; revised 4 Sep 2009; accepted 8 Sep 2009; published 21 Sep 2009

field distribution of the TE mode and the $\boldsymbol{E}_z$ field distribution of the TM mode, respectively. TM-polarized light is concentrated in the air region, satisfying the continuity condition on the normal component of the displacement field at the silicon-air interface [24, 25].

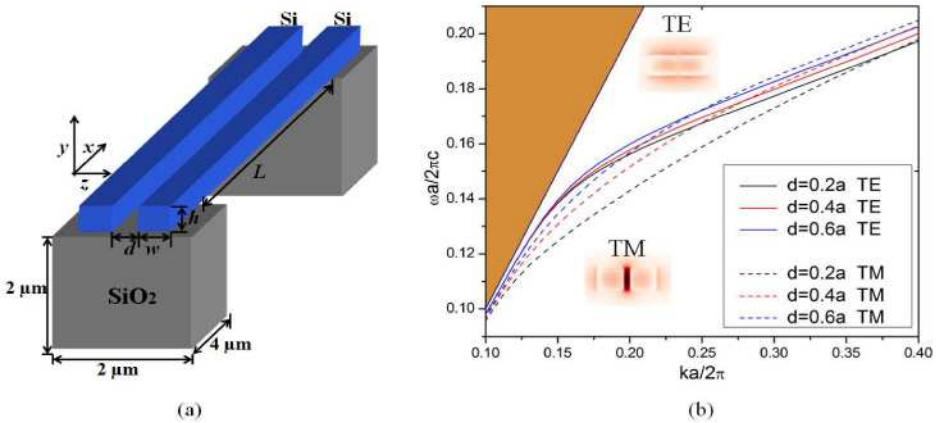

Fig. 1. (a) Two coupled Si waveguides, each with cross section $w \times h$ separated by a distance d, rest on a SiO2 substrate with a free-standing section of length L. (b) Dispersion relation for the lowest-frequency TE mode (solid lines) and TM mode (dashed lines) of the coupled waveguides for several separations. Insets respectively show the $\boldsymbol{E}_y$ field distribution of the TE mode and the $\boldsymbol{E}_z$ field distribution of the TM mode with d=0.2a at frequency $\omega a/2\pi c$=0.18 (darker shades correspond to larger magnitudes of the electric field at a snapshot in time). The yellow region shows the light cone.

TE and TM modes have different propagation characteristics. The group birefringence is obtained by taking the difference between the group indices $\Delta n_g = n_g^{TE} - n_g^{TM}$, where n_g^{TE} and n_g^{TM} are the group indices of the TE and TM modes, respectively, at a fixed frequency ω. The group index is calculated as $n_g^{TE,TM} = c/(d\omega/dk)^{TE,TM}$ and is proportional to the reciprocal of the slope of the dispersion curve in Fig. 1(b). Phase birefringence is $\Delta n_p = n_p^{TE} - n_p^{TM}$, where n_p^{TE} and n_p^{TM} respectively denote the phase indices of the TE and TM modes at a fixed frequency ω. The phase index is calculated by $n_p^{TE,TM} = ck^{TE,TM}/\omega$. For small separation ($d$=0.2$a$), the optical fields in the two strips are strongly coupled. The bands for TE and TM light are significantly different. It can be inferred from the figure that group and phase birefringence are relatively large in some frequency ranges. If the separation is increased (d=0.4a or d=0.6a), the coupling between the strips becomes weaker, and the dispersion curves of TE and TM modes are closer to one another. Group and phase birefringence are reduced. For infinite waveguide separation (d=∞), no coupling occurs. Modes propagate independently in each single-strip waveguide. The bands of the TE and TM modes overlap, and the birefringence vanishes.

Coupling between the strips gives rise to an optical force on the waveguides [1]. The force depends on the frequency of light propagating in the waveguides (pump frequency), the incident power, and the waveguide separation. For fixed incident power and waveguide separation, we optimize the force magnitude by selecting an appropriate frequency and polarization of pump light. As in previous work [1], we calculate the force as a function of frequency using the Maxwell Stress Tensor formulation [26], which gives the force as an integral expression over the electric and magnetic fields of the waveguides. We solve for the full vectorial fields using the MIT Photonic Bands package [23]. Figure 2(a) shows the force magnitude as a function of the pump frequency for a waveguide separation d = 0.35a. We focus on the dimensionless frequency ($\omega a/2\pi c$) range from 0.15 to 0.21. For lower

#113783 - $15.00 USD Received 7 Jul 2009; revised 4 Sep 2009; accepted 8 Sep 2009; published 21 Sep 2009

frequencies, the bands are closer to the light line, and the waveguide modes spread out in the surrounding air. For frequencies larger than 0.21, there are at least two symmetric TE (or TM) modes for a single frequency, resulting in multimodal coupling. We compare the force induced by TM (red) and TE (black) modes. The strongest force is obtained for TM-polarized light at frequency $\omega_p a/2\pi c$=0.165. According to Eq. (1) in [1],

$$F = -\frac{1}{\omega}\frac{d\omega}{d\xi}\bigg|_k U \tag{1}$$

which indicates the mechanical force F is proportional to the derivative of frequency ω with respect to waveguide separation ξ for conserved wave vector k and energy U. In Fig. 1(b), we see that for a fixed wave vector k, if the waveguide separation is reduced, the frequency of the TM mode changes more than that of the TE mode. Therefore, the TM mode induces a bigger force. In the remainder of the paper, we will assume that TM pump light is used to exert force on the waveguides and deform their shape. We will consider the effects of the deformation on the propagation of both TE and TM signal light.

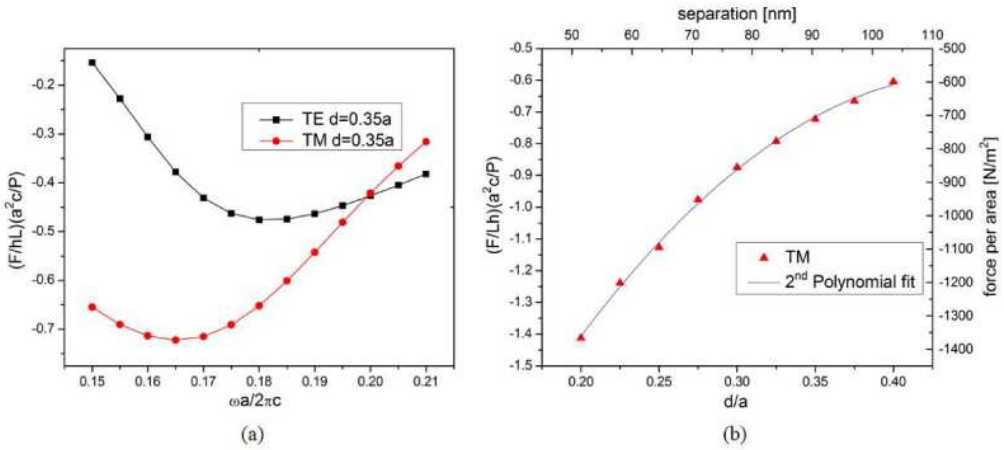

Fig. 2. (a) Normalized force per unit area for the lowest-frequency TE (red) and TM (black) modes as a function of pump light frequency, at fixed separation d=0.35a. (b) Force per unit area as a function of separation (red triangles), at optimized frequency $\omega_p a/2\pi\ c=a/\lambda_p$=0.165. The right and top axes are in physical units with incident power P=20 mW, w=h=a=263.5nm, and L=30 μm. The blue solid line is the second-order polynomial fit of the force per unit area.

On the left and bottom axes of Fig. 2(b), we plot the dimensionless force per unit area $(F/Lh)(a^2c/P)$ as a function of the normalized separation d/a at the optimized frequency $\omega_p a/2\pi c$=0.165. The symbol c represents the speed of light in vacuum, and P denotes the incident power. Substituting the values P=20mW, w=h=a=263.5nm, and pump wavelength λ_p=1597nm, we plot the force per unit area versus separation on the right and top axes in Fig. 2(b).

We perform FEM numerical simulations to calculate the deformation of waveguides caused by the attractive force using COMSOL Multiphysics software [22]. We simulate the full three-dimensional structure consisting of two silicon waveguides, each with a square cross section of 263.5×263.5nm^2 and a length of 30μm. The ends of each waveguide are fixed. We assume an initial waveguide separation d=0.35a=92.2nm. The waveguide ends are fixed at this separation. The optical force pulls the waveguides toward one another. As the waveguides deform, the magnitude of the force increases. We use a second-order polynomial to approximate the force density for waveguide separation d between 0.2a and 0.35a, as shown by the solid blue line in Fig. 2(b). For the mechanical parameters of Si, we take the mass density ρ=2330 kg/m^3 and Young's modulus E=131GPa. Figure 3 shows the waveguide

#113783 - $15.00 USD Received 7 Jul 2009; revised 4 Sep 2009; accepted 8 Sep 2009; published 21 Sep 2009

deformation as a function of position along the waveguides with L=30μm, w=h=a=263.5nm, d=92.2nm, and P=20mW. The biggest displacement (9 nm) is obtained at the waveguide center. The smallest distance between the two waveguides is 74.2nm. Following [27], we estimate the van der Waals force per unit area to be approximately 25N/m^2 between two parallel infinitely extended Si slabs of thickness 263.5nm and separation 74.2nm. For this separation, the van der Waals force is several orders of magnitude less than the optically-induced force and can therefore be neglected. It is interesting to note that experiments have been done in a similar coupled system, showing that pulsed light can obtain a comparable displacement at a lower power of a few milliwatts [10].

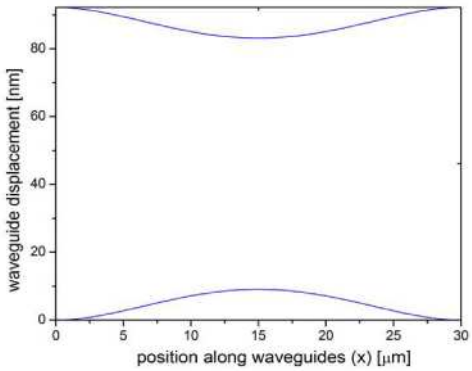

Fig. 3. Displacement of the suspended section of each waveguide as a function of position along the waveguide. The cross-sectional dimension is w=h=a=263.5nm, the initial waveguide separation is d=0.35a ≈92.2nm, the pump frequency is $\omega_p a/2\pi c = a/\lambda_p$=0.165, the incident power is P=20 mW, and the suspended length is L=30 μm. Note that the x and y axes differ in scale.

3. Tunable phase birefringence

The phase birefringence is a function of the separation between the strips. We consider the birefringence experienced by light at a signal frequency ω. We assume that the signal power is much weaker than the pump power, such that the optical force due to the signal can be neglected. We calculate the phase birefringence Δn_p as a function of dimensionless signal frequency $\omega a/2\pi c$ for different separations from 0.2a to 0.35a, as shown in Fig. 4(a). The arrow indicates that at signal frequency $\omega_s a/2\pi c$=0.17 (a=263.5nm, λ_s=1550 nm), the absolute value of Δn_p increases as the waveguide separation decreases.

When the waveguides are deformed by an attractive optical force, the separation varies along the waveguide length as shown in Fig. 3. The propagating signal experiences a spatially-varying birefringence. Figure 4(b) shows the phase birefringence as a function of position along waveguides for a CW pump at frequency $\omega_p a/2\pi c$=0.165 with power P=20mW. For zero pump power (zero force), the waveguides are parallel and the birefringence is ≈0.067 throughout the whole free-standing section. With the pump on, the birefringence is increased. The maximum value is approximately 0.093 at the waveguide center. The difference between the maximum and the minimum of $\left|\Delta n_p\right|$ is 0.026.

#113783 - $15.00 USD Received 7 Jul 2009; revised 4 Sep 2009; accepted 8 Sep 2009; published 21 Sep 2009

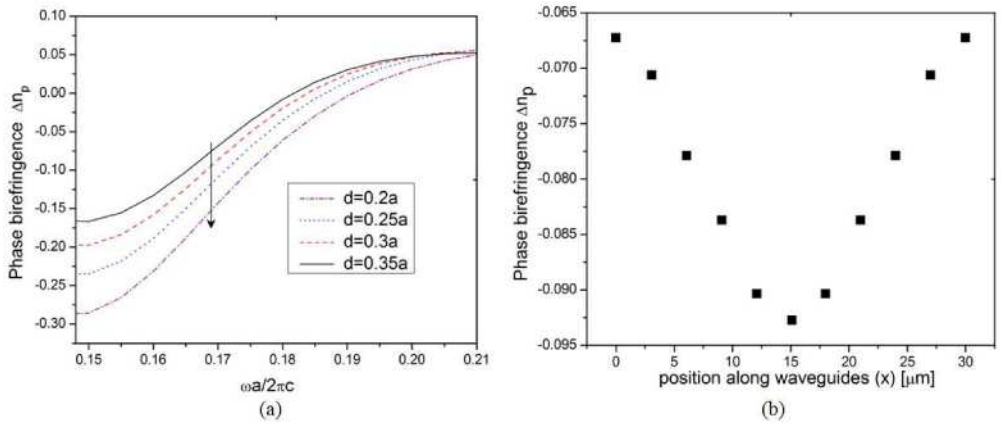

Fig. 4. (a) Phase birefringence Δn_p as a function of signal frequency in the coupled waveguides with varying separations. The arrow shows that at a frequency $\omega_s a/2\pi c$=0.17, the absolute value of Δn_p increases as the waveguide separation d decreases. (b) Phase birefringence Δn_p as a function of position along the waveguides. The initial separation is d=0.35a≈92.2nm. The attractive force is induced by CW pump light at frequency $\omega_p a/2\pi c = a/\lambda_p$=0.165 and power P=20mW. The difference between the maximum and the minimum of $|\Delta n_p|$ is 0.026.

3.1 Tunable relative phase-shift

A potential application of the system is to dynamically adjust the relative phase shift between TE and TM modes. The total phase shift between TE and TM modes is calculated as:

$$\Delta\phi = \int_0^L \left| k^{TE}(x) - k^{TM}(x) \right| dx = \frac{\omega}{c} \int_0^L \left| n_P^{TE} - n_P^{TM} \right| dx = \frac{2\pi}{\lambda_S} \int_0^L \left| \Delta n_P \right| dx \qquad (2)$$

The phase shift in two parallel waveguides with a separation of 92.2 nm is estimated to be 2π×30μm×0.067/1.55 μm ≈2.59π, equal to 0.59π modulo 2π. When we input CW pump light with a power of 20 mW, the waveguides deform and the phase shift is changed to 3.11π, or 1.11π modulo 2π. The tuning range is about 0.5π. If we reduce the waveguide length to 23.05 μm, the total relative phase shift of a linear signal is 2π at the output of the un-deformed device. We plot the relative phase difference (phase difference modulo 2π) as a function of input pump power, as shown by black squares in Fig. 5. By increasing the pump power, the phase difference can be adjusted from 0.12π to 0.51π. Taking the pump power to be about 67 mW, we obtain a total relative phase shift of 0.5π. Thus, an incoming signal of linear light whose *E*-field is at 0.25π to the *y* (or *z*) axes will emerge from the device circularly polarized.

We note that a variety of approaches exist for polarization control in fiber [28] and on-chip microphotonic systems [29–32]. In microphotonic systems in particular, polarization rotators have been designed based on tapered waveguide cores [29] and asymmetric waveguides [30–32]. Ref [33]. presented a linear-to-circular polarization converter based on a high-Q dielectric microring resonator. In contrast to these approaches, we take advantage of mechanical motion to yield a widely tunable phase shift that is also broadband (non-resonant) in response. For a device with fixed length, the phase birefringence and relative phase shift can be dynamically adjusted by varying pump light power. Unlike other polarization control schemes using semiconductor optical amplifiers [34, 35] or electrooptic materials, our approach is fully compatible with SOI materials systems.

#113783 - $15.00 USD Received 7 Jul 2009; revised 4 Sep 2009; accepted 8 Sep 2009; published 21 Sep 2009

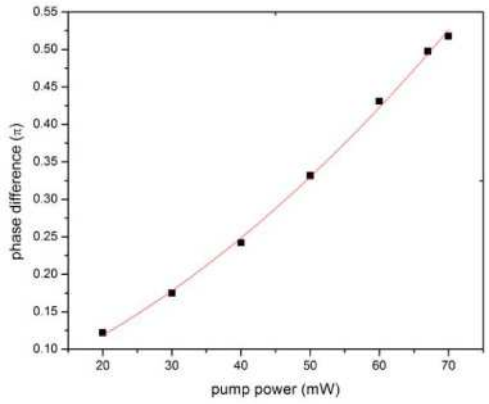

Fig. 5. Tuning the relative phase shift by increasing CW pump power from 20mW to 70mW (black squares). The waveguide length is 23.05μm. The red line is a 2nd –order polynomial fit of the phase shift. A power of approximately 67mW yields a 0.5π phase difference.

3.2 Other tuning configurations

The dependence of phase birefringence on separation can be changed by altering the waveguide cross section. Figure 6 (a) depicts the birefringence versus signal frequency in two a×2a waveguides. The arrow indicates that the value of Δn_p decreases with decreasing separation for frequencies from 0.11 to 0.16. The tuning trend is opposite from that in the system with two square waveguides. We can understand the trend by considering two extreme cases. For zero separation, light propagates in a square waveguide of cross section 2a×2a, which has no birefringence due to spatial symmetry. For infinite separation, light propagates in a single rectangular waveguide asymmetric with respect to the y and z axes, which has large birefringence. Figure 6 (b) shows another waveguide structure with a cross section a×0.5a. The effective index of the TE mode is less than that of the TM mode. The absolute value of Δn_p increases with decreasing separation for frequencies from 0.20 to 0.25.

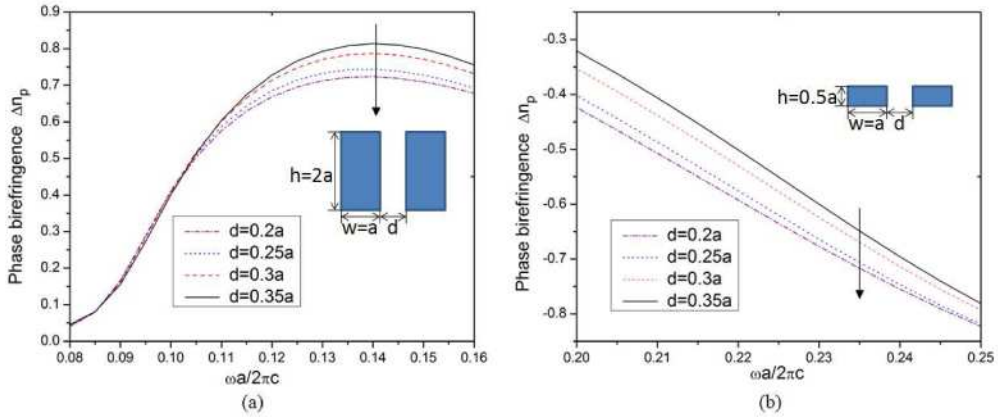

Fig. 6. Phase birefringence Δn_p as a function of signal frequency in the two-waveguide system with varying separations. (a) The cross section of each waveguide is a×2a. The arrow shows that Δn_p decreases with decreasing separation. (b) The cross section of each waveguide is a×0.5a. The absolute value of Δn_p increases with decreasing separation.

4. Tunable group birefringence

The group birefringence also depends on waveguide separation and can be tuned by deforming the waveguides via an optical force. We plot the group birefringence Δn_g as a function of dimensionless signal frequency $\omega a/2\pi c$, for different separations from 0.2a to

#113783 - $15.00 USD Received 7 Jul 2009; revised 4 Sep 2009; accepted 8 Sep 2009; published 21 Sep 2009

0.35a in Fig. 7(a). The birefringence increases with decreasing separation. The arrow indicates that the group birefringence Δn_g increases fastest at a frequency $\omega_s a/2\pi c$=0.17 (a=263.5nm, λ_s=1550 nm). We consider deformation due to an attractive optical force for CW pump light at frequency $\omega_p a/2\pi c$=0.165 and power P=20 mW, as above. Figure 7(b) shows the group birefringence of signal light as a function of length along the waveguides for L=30μm. The initial value 1.09 corresponds to the birefringence of the undeformed waveguides. The peak of the birefringence is approximately 1.22 at the waveguide center. The difference between the maximum and the minimum of $|\Delta n_p|$ is 0.13.

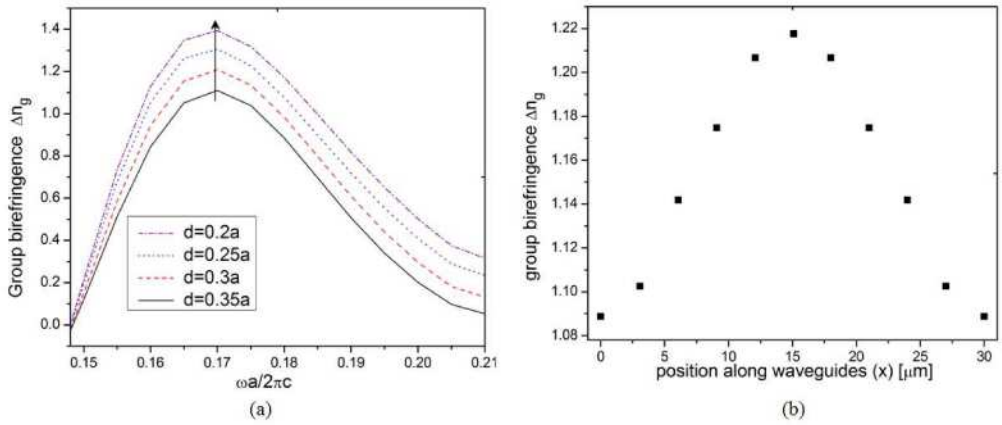

Fig. 7. (a) Group birefringence Δn_g as a function of signal frequency, in the coupled waveguides with varying separations. The arrow shows that as the waveguide separation d increases, the group birefringence Δn_g increases fastest at a frequency $\omega_s a/2\pi c$=0.17. (b) Group birefringence Δn_g as a function of position along the waveguides. The waveguides are deformed by an attractive force induced by a CW pump at frequency $\omega_p a/2\pi c = a/\lambda_p$=0.165, with a power P=20mW. The difference between the maximum and the minimum of Δn_g is 0.13.

The system can be used to tune the polarization-selective delay between TE and TM pulses. The delay is tuned by adjusting the pump power. The differential time delay between TE and TM pulses is calculated as:

$$\Delta t = \int_0^L (\frac{1}{v_g^{TE}} - \frac{1}{v_g^{TM}})dx = \frac{1}{c}\int_0^L (n_g^{TE} - n_g^{TM})dx = \frac{1}{c}\int_0^L \Delta n_g dx \qquad (3)$$

For two parallel waveguides without deformation, the differential time delay is 1.09×30μm/3×10^8=109fs. By inputting CW pump light at a power of 20mW, we increase the differential time delay to 115fs.

If we consider applications where the pulse width is comparable to the tunable delay range, we can take the pulse width T=6fs. We can estimate the dispersion length as $L_D = T^2/\beta_2$ [36], where the dispersion coefficient $\beta_2 = d^2k/d\omega^2$ is 2.2×10^{-25} s^2/m. L_D is around 164 micrometers, much larger than the waveguide length. We can thus assume that minimal distortion occurs due to propagation through the 30μm long suspended section.

The tuning range can be increased by increasing the pump power. The tuning range can also be increased by fabricating longer suspended sections, which deform more easily for fixed power, or by fabricating multiple suspended sections in series.

Note that this analysis also applies to vibrating waveguides actuated by pulsed pump light [10]. The dynamic system experiences similar displacement as the static system for much smaller pump powers. While the waveguide beam vibrates in a period of a few hundred nanoseconds, the transmission time of a signal pulse through the 30μm waveguide is on the order of a femtosecond. The beam can thus be treated as static in the calculation of time delay, provided that the signal pulse is much shorter than the vibration period in time.

#113783 - $15.00 USD Received 7 Jul 2009; revised 4 Sep 2009; accepted 8 Sep 2009; published 21 Sep 2009

5. Thermal effects

In addition to optical forces, thermal effects may also contribute to waveguide deformation. The waveguides absorb propagating light, experience thermal expansion, and are mechanically deformed. We performed FEM (finite element method) simulations to calculate the displacement caused by the photo-thermo-mechanical effect using COMSOL Multiphysics software. We considered two silicon waveguides with identical cross section $263.5\times263.5\text{nm}^2$ and separation 92.2nm sitting on top of a silicon dioxide substrate, as shown in Fig. 1(a). The free-section length of the beams is 30μm. We used a similar simulation method to that introduced in the supplementary methods of [10]. The beams are assumed to be thermally isolated, except where they contact the substrate. The boundaries of the silicon dioxide substrate are assumed to be of constant temperature 300K. The absorption constant of silicon α is estimated to be 0.0079cm^{-1} at 1.597μm pump wavelength by using the equation $\alpha=4\pi k/\lambda$ and the value of the extinction coefficient k in [37]. With 20mW incident optical power, the absorbed power is approximately 0.474μW. After using the RF module to solve for the pump mode profile, we define a resistive heating power of 0.474μW as the heating source in the thermal module. We obtain a calculated temperature profile that shows a peak temperature T-300=0.097K near the center of the beams. The thermal simulation is followed by a mechanical simulation to solve for the mechanical stress that results from the thermal load. We are primarily concerned with the mechanical displacement in the z direction, which may introduce inaccuracy into the birefringence tuning. A peak z-displacement of 0.392pm is reached at the waveguide center. The peak displacement in the y-direction was <5pm. The thermally induced displacement is thus negligible compared with the displacement due to the optical force of 9nm.

Considering that the thermo-optical coefficient $\partial n/\partial T=1.86\times10^{-4}\text{K}^{-1}$ for silicon, we estimate that the refractive index change due to our calculated temperature increase is on the order of 10^{-5}, which is far smaller than the index change caused by optomechanical deformation.

We conclude that thermal effects can be neglected in the system studied here, in agreement with the conclusions found in [10] for a similar experimental system.

6. Conclusion

In this work, we present an optomechanically-controlled system which resembles a suspended one-slot waveguide with adjustable slot width depending on the optical force. The change in slot width corresponds to a change in the symmetry of the cross-section of the device, and therefore tunes both phase and group birefringence. We optimize the polarization and frequency of continuous pump light to obtain a considerable force at low operating power. The deformed 30μm waveguide shows a maximum displacement of about 9 nm at the center for a power of 20mW. Correspondingly, the phase (group) birefringence at the waveguide center is different from that at the clamped ends by 0.026 (0.13), which is larger than previous records. When used to tune the relative phase of two orthogonally polarized light signals, the device has a tuning range of around π/2. If the orthogonally polarized components have identical amplitudes, it is possible to rotate the polarization state from linear to circular in a distance of 30μm. We show further that the dependence of phase birefringence on separation can be changed by altering the waveguide cross section. When used as a polarization-dependent tunable delay element, the two-waveguide system has a tuning range of 6fs. We note that the birefringence tuning trends studied here apply not only to a two-beam system deformed by an optical force, but also by other actuation methods, including static electrostatic forces used in micro-electro-mechanical systems (MEMS).

In the future, the potential to tune birefringence via an optical force may be applied to design novel microring resonator systems. Waveguide-coupled microrings exhibit a strong (static) birefringence, which can be used to realize polarization converters and polarization-

#113783 - $15.00 USD Received 7 Jul 2009; revised 4 Sep 2009; accepted 8 Sep 2009; published 21 Sep 2009

sensitive delay devices [38–40]. Recent experiments have shown that the separation between vertically-stacked microrings can be adjusted via optical forces [13]. This capability may in the future be exploited to design highly-tunable birefringent devices along similar lines as studied here.

Acknowledgements

Computing resources were provided by the USC Center for High Performance Computing and Communications. Jing Ma was funded by a Viterbi Fellowship. Michelle Povinelli was funded by USC WiSE Jr. Gabilan and Powell Awards.

#113783 - $15.00 USD Received 7 Jul 2009; revised 4 Sep 2009; accepted 8 Sep 2009; published 21 Sep 2009